Optical Inter-Satellite Link Analysis

Linzhe (Jeremy) Wang

Winter 2024

Contents

List of Figures

List of Tables

1 Introduction

This project focuses on analyzing the performance of optical inter-satellite links. Its objective is to develop and analyze a comprehensive system model tailored for these links. The model meticulously accounts for a broad range of factors crucial to satellite operations, including atmospheric attenuation, satellite velocity, Doppler shift, and the varying elevation angles encountered throughout satellite orbits. By integrating mathematical models for path loss, Doppler shift, atmospheric attenuation, and link margin into the simulation, the project aims to provide an in-depth understanding of the dynamics involved in optical inter-satellite communication.

1.1 Motivation

The advancement of SpaceX's reusable rocket technology has significantly reduced the costs of delivering payloads to orbit, sparking renewed interest in satellite applications, especially in optical inter-satellite links. This interest is particularly pronounced in networks of Low Earth Orbit (LEO) satellites. Due to their closer proximity to Earth, these satellites offer shorter path lengths and reduced round-trip times (RTT), advantages that have likely fueled research into refining satellite link analysis and simulation. The project aims to conduct a detailed examination of critical factors like atmospheric attenuation, satellite velocity, Doppler shift, and the impact of varying elevation angles on link performance. These considerations are vital for optimizing next-generation satellite communication systems.

1.2 Related Work

Current research in the field of LEO satellite communication has made significant strides towards understanding and optimizing link budget analysis, a key factor in enhancing the reliability and efficiency of communications. Recent studies have notably contributed innovative methodologies for link budget analysis that accommodate the dynamic nature of LEO satellites. A significant development is the novel approach of modeling the variability of the elevation angle, θ_E, as a gamma-distributed random variable. This methodology markedly enhances the precision of predicting received power (P_{rx}) statistics, thereby enabling more accurate estimations of power levels above or below certain thresholds [1]. This advanced analytical framework not only underscores the evolving complexity of LEO satellite communications but also highlights ongoing efforts to refine link budget analysis, aiming for improved performance and reliability in space-based communication networks.

Another notable study offers a comprehensive evaluation of link budget for nano-satellite communications within LEO, shedding light on the crucial balance between data rates and power efficiency. This research advocates for the utilization of the UHF band, highlighting its effectiveness in minimizing RF propagation attenuations while adeptly managing the impacts of Doppler shift [2].

Further investigations into the realm of satellite communications reveal that transmission power requirements for both optical inter-satellite links and uplink/downlink communications inherently increase with link distance. However, a fascinating discovery within these studies is the inverse relationship between transmission power and the elevation angle for uplink and downlink transmissions [3]. This relationship suggests a promising avenue

for optimizing satellite communications by adjusting the elevation angle to reduce power requirements, thereby enhancing the overall efficiency of the link budget.

Additionally, the exploration of Frequency Reuse (FR) schemes within GEO/LEO New Radio systems, particularly within the Ka-band, underscores the effectiveness of FR3 and FR4 schemes in boosting system performance [4]. This advancement is achieved without the need for complex interference management strategies such as MMSE-IRC, highlighting the potential of FR schemes in significantly enhancing link budget performance in Non-Terrestrial Networks (NTNs).

Lastly, the feasibility study on the use of E-band frequencies for establishing high-speed broadband communication links between LEO satellites and ground stations represents a groundbreaking exploration. The study's realistic link budget calculations suggest the potential to achieve data rates up to 5.0 Gbit/s with high availability (98.39%), under specific conditions [5]. This finding opens up new possibilities for achieving unparalleled data transmission speeds in LEO satellite communications.

Collectively, these studies contribute to a deeper understanding and substantial improvement of link budget equations for satellite communication systems. By addressing various aspects of the link budget analysis, from power efficiency and frequency band selection to frequency reuse schemes and high-speed data transmission, this body of research lays the groundwork for future advancements in satellite communication technology, ensuring better performance and reliability in space-based networks.

2 System Model

The analysis of optical inter-satellite links demands a propagation model that accurately embodies the unique conditions of satellite operation. It must consider factors such as atmospheric attenuation, the satellite's relative proximity to Earth, high velocity, resulting Doppler shift, and the changing elevation angles encountered during the satellite's orbit. Accordingly, the section addresses mathematical models for optical inter-satellite link, path loss, Doppler shift, atmospheric attenuation, and link margin used in the simulation.

2.1 Optical Inter-Satellite Link

A link model represents a breakdown of the key power gains and losses (typically measured in dB) within a communication system, extending from a transmitter to a receiver. An optical inter-satellite link refers to the connection between two satellites, where the propagation medium is the vacuum of space, given that these links are established between satellites positioned in space [6].

$$P_R = P_T \eta_T \eta_R G_T G_R L_T L_R L_{PS} \tag{1}$$

- P_R = received power in Watts
- P_T = transmitted power in Watts
- η_T = optics efficiency of the transmitter
- η_R = optics efficiency of the receiver

- G_T = transmitter gain
  - $G_T = \frac{16}{(\Theta_T)^2}$
  - Θ_T = full transmitting divergence angle in radians
- G_R = receiver gain
  - $G_R = \left(\frac{D_R \pi}{\lambda}\right)^2$
  - D_R = receiver's telescope diameter in mm
- L_T = transmitter pointing loss
  - $L_T = \exp\left(-G_T(\theta_T)^2\right)$
  - θ_T = transmitter pointing error in radians
- L_R = receiver pointing loss
  - $L_R = \exp\left(-G_R(\theta_R)^2\right)$
  - θ_R = receiver pointing error in radians
- L_{PS} = free-space path loss for the optical link between satellites

2.2 Path Loss

A widely used path loss model for satellite is the Free Space Path Loss (FSPL) model, particularly because it suits the line-of-sight communication typically found in satellite links. The equation, named after the radio pioneer Harald T. Friis [7], is given by

$$L_{PS} = \left(\frac{\lambda}{4\pi d_{SS}}\right)^2 \tag{2}$$

- λ = carrier wavelength
- d_{SS} = distance between satellites. (lies in the far-field region of the antennas, the rule of thumb being $d_{SS} \geq 2\frac{d^2}{\lambda}$, where d is the largest physical dimension of either antenna)

For calculation purposes, VHF = 145 MHz, UHF = 435 MHz, and L-band = 1 GHz have been selected as the operating frequencies. Figure 1 suggests that higher frequency communication experiences greater free space loss, and thus requires more transmission power.

- VHF (Very High Frequency):
  - Frequency Range: 30 MHz to 300 MHz
  - Applications: FM radio broadcasting, television broadcasting, two-way land mobile radio systems (such as walkie-talkies and marine radio), and air traffic control communications
- UHF (Ultra High Frequency):

  - Frequency Range: 300 MHz to 3 GHz
  - Applications: television broadcasting, mobile phones, GPS, Bluetooth, Wi-Fi, and two-way radios

- L-band:
  - Frequency Range: 1 GHz to 2 GHz
  - Applications: satellite communications, including mobile satellite communications, GPS, and aircraft surveillance systems

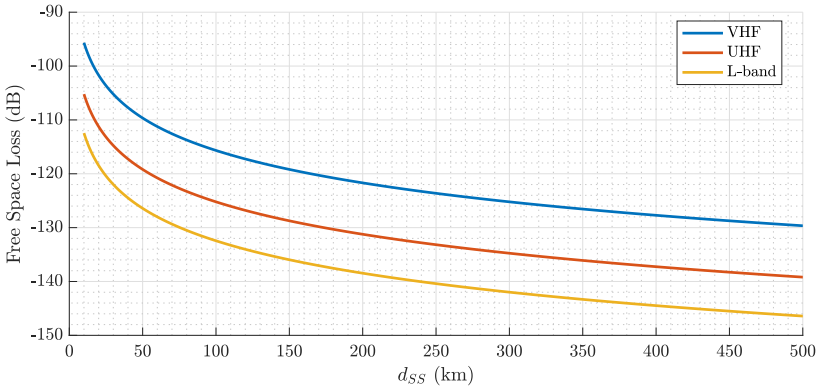

Figure 1: Free space loss for chosen frequencies in VHF, UHF, and L-band.

2.3 Doppler Shift

Doppler shift, also known as the Doppler effect, is a change in the frequency or wavelength of a wave in relation to an observer who is moving relative to the wave source. In different orbits, the Doppler shift can be significant due to the high velocity of the satellites. When a satellite has a relative velocity of V_c along the line of sight, the frequency shift of the received signal is given by

$$f_{dopp} = \frac{V_r \cdot f}{c} \tag{3}$$

- f = carrier frequency
- V_r = radial component of the circular velocity of the satellite

Assuming that the orbit is circular and the Earth is perfectly spherical, the circular velocity is given by

$$V_c = \sqrt{\frac{\mu}{R_E + h_S}} \tag{4}$$

- μ = gravitational constant of the Earth
- h_S = altitude of the satellites

The relative velocity, V_r, can be decomposed into two components in relation to the ground station: the tangential velocity and the radial velocity. The radial component can be determined using the equation below:

$$V_r = V_c \sin \beta \tag{5}$$

$$\frac{\sin(90 + \theta_E)}{R_E + h_S} = sin\left(\frac{\beta}{R_E}\right) \tag{6}$$

- θ_E = elevation angle

Therefore, the Doppler shift frequency is derived by substituting eq. 5 and eq. 6 in eq. 3:

$$f_{dopp} = \frac{V_c f}{c} \frac{R_E \cos \theta_E}{R_E + h_S} \tag{7}$$

Figure 2 suggests that the Doppler shift increases with frequency, resulting in a deviation of up to 56 kHz for the L-band. An elevation angle of 90° indicates that the satellite is directly above the ground station. Understanding the Doppler shift is crucial for accurate link budget calculations.

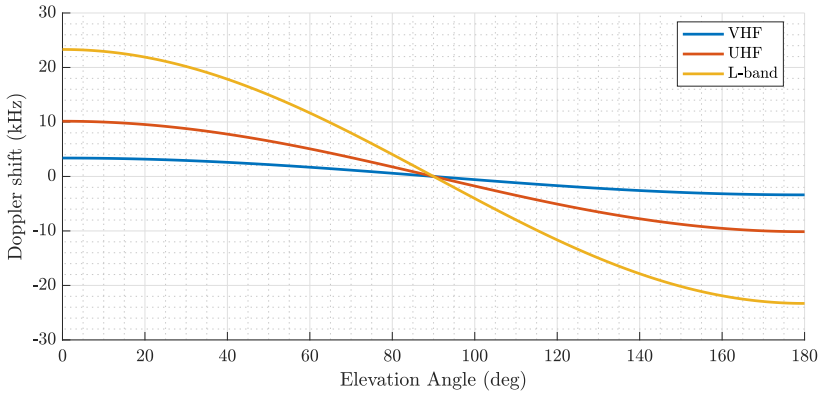

Figure 2: Doppler shift versus elevation angle in VHF, UHF, and L-band.

2.4 Atmospheric Attenuation

Optical uplink and downlink communications between satellites and ground stations are subject to attenuation due to atmospheric conditions. Scattering, which involves the redirection of beam energy by particles along the beam's propagation path, significantly contributes to this attenuation. This project focuses on Mie scattering and geometrical scattering as the main factors for atmospheric attenuation, as they are the primary sources of beam scattering and, consequently, beam fading within the atmosphere.

Thus, the received power with atmospheric attenuation is given by

$$P_R = P_T \eta_T \eta_R G_T G_R L_T L_R L_A L_{PG} \tag{8}$$

- L_A = atmospheric attenuation loss

- L_{PG} = free space path loss for links between ground stations and satellites [8]

The free space path loss, L_{PG}, can be expressed based on slant distance [9], (i.e., the distance between a ground station and a satellite) as

$$L_{PG} = \left(\frac{\lambda}{4\pi d_{GS}}\right)^2 \tag{9}$$

$$d_{GS} = R\left(\sqrt{\left(\frac{R+H}{R}\right)^2 - (\cos(\theta_E))^2} - \sin(\theta_E)\right) \tag{10}$$

- θ_E = elevation angle
- $R = R_E + h_E$
- $H = h_S - h_E$
  - R_E = radius of the Earth and is considered as 6378.1 km
  - h_E = height of ground station and is located at h_E km above the mean sea level
  - h_S = altitude of the satellites

2.4.1 Mie Scattering

Mie scattering takes place when atmospheric particles have a diameter that matches or exceeds the wavelength of the optical beam. This phenomenon is predominantly observed in the lower atmosphere, where larger particles are more prevalent, with microscopic water particles being the primary contributors. The subsequent formula is adept at accurately modeling the Mie scattering effect, specifically for ground stations situated at altitudes ranging from 0 to 5 km above mean sea level:

$$\rho = a(h_E)^3 + b(h_E)^2 + c(h_E) + d \tag{11}$$

- ρ = denotes the extinction ratio
- a, b, c, d = wavelength dependent empirical coefficients
  - $a = -0.000545\lambda^2 + 0.002\lambda - 0.0038$
  - $b = 0.00628\lambda^2 - 0.0232\lambda + 0.00439$
  - $c = -0.028\lambda^2 + 0.101\lambda - 0.18$
  - $d = -0.228\lambda^3 + 0.922\lambda^2 - 1.26\lambda + 0.719$

The atmospheric attenuation due to Mie scattering [10], can be expressed as

$$I_m = \exp\left(\frac{-\rho}{\sin(\theta_E)}\right) \tag{12}$$

2.4.2 Geometrical Scattering

Geometrical scattering models the attenuation caused by atmospheric conditions near the Earth's surface, such as fog or dense clouds. The model includes the following formula to illustrate the impact of geometrical scattering.

$$V = \frac{1.002}{(L_W N)^{0.6473}} \tag{13}$$

- V = visibility in km
- L_W = liquid water content in $\frac{g}{m^{-3}}$
- N = cloud number concentration in cm^{-3}

The attenuation coefficient θ_A can be expressed as

$$\theta_A = \left(\frac{3.91}{V}\right)\left(\frac{\lambda}{550}\right)^{-\phi} \tag{14}$$

- ϕ = particle size related coefficient according to Kim's model [11]
- The Beer-Lambert law [12], is given as $I(z) = \exp(-\mu z)$
  - μ = attenuation coefficient that depends on wavelength
  - z = distance of the transmission path

For geometrical scattering, the atmospheric attenuation can be expressed using the Beer-Lambert law as

$$I_g = \exp\left(-\theta_A d_A\right) \tag{15}$$

- d_A = distance of the optical beam through the troposphere layer of the atmosphere over which it encounters geometrical scattering
  - $d_A = (h_A - h_E)\csc(\theta_E)$
  - h_A = height of the troposphere layer of atmosphere in km

The atmospheric attenuation loss considering both Mie scattering and geometrical scattering [13] can then be calculated as

$$L_A = I_m I_g = \exp\left(\frac{-\rho}{\sin(\theta_E)}\right)\exp\left(-\theta_A d_A\right) \tag{16}$$

2.5 Link Margin

The efficacy of an optical communication system is often measured using metrics such as link margin and bit error rate, among others. Link margin is the ratio between the power of the signal received and the minimum necessary signal power to attain a certain bit error rate at a predetermined data rate. This margin is essential for compensating unforeseen

losses and interferences, and it must remain positive to ensure the received signal is correctly interpreted. The calculation for link margin is represented by the following equation:

$$LM = \frac{P_R}{P_{req}} \tag{17}$$

- P_R = received power in mW
- P_{req} = receiver sensitivity in mW [8]

3 Results

The section presents the simulation results using the system model discussed in Section 2. The analysis aims to investigate the behavior of transmission power due to different factors, such as inter-satellite link distance, slant distance, elevation angle, and link margin.

3.1 Optical Inter-Satellite Link vs. Transmission Power

The optical link model parameters summarized in Table 1 are considered for evaluating optical inter-satellite links as well as uplink and downlink communications. These parameters are utilized in actual optical satellite communication systems. The link transmission power is computed using equations (1) and (2), which are based on the parameters listed in Table 1. Figure 3 suggests that the required transmission power increases as the link distance increases.

Parameter	**Symbol**	**Units**	**Value**
Laser wavelength [14]	λ	nm	1550
Transmitter optical efficiency [15]	η_T		0.8
Receiver optical efficiency [15]	η_R		0.8
Data rate [16]	R_{data}	Gbps	10
Receiver telescope diameter [14]	D_R	mm	80
Transmitter pointing error [15]	θ_T	μrad	1
Receiver pointing error [15]	θ_R	μrad	1
Full transmitting divergence angle [14]	Θ_T	μrad	15
Receiver sensitivity [16]	P_{req}	dBm	-35.5
Bit error rate [16]			10^{-12}
Link Margin	LM	dB	3

Table 1: Link model parameters

3.2 Slant Distance vs. Transmission Power

The computation of optical uplink/downlink transmission power incorporates parameters related to atmospheric attenuation, as summarized in Table 2. Equations (11) and (12) are employed to calculate Mie scattering, I_m, which is influenced by the ground station altitude, h_E, elevation angle, θ_E, and wavelength, λ. Geometrical scattering, I_g, is determined according to equations (13) to (15). Subsequently, atmospheric attenuation loss, L_A, is derived

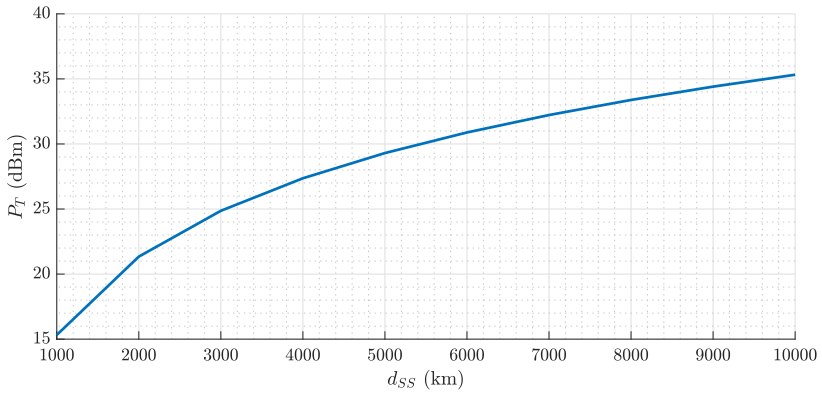

Figure 3: Link distance vs. transmission power

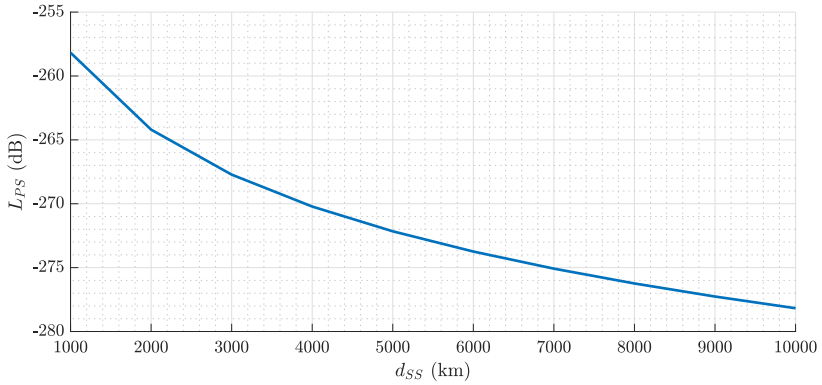

Figure 4: Link distance vs. path loss

using equation (16), and P_T for optical uplink/downlink is calculated as presented in Table 3 and Figure 5.

Parameter	Symbol	Units	Value
Ground station height [13]	h_E	km	1
Thin cirrus cloud concentration [11]	L_w	cm^{-3}	0.5
Liquid water content [11]	N	g/m^3	3.128×10^{-4}
Partial size coefficient [13]	ϕ		1.6
Elevation angle [17]	θ_E	degree	40
Troposphere layer height [18]	h_A	km	20

Table 2: Atmospheric attenuation parameters

3.3 Elevation Angle vs. Transmission Power

Both Mie and geometrical scatterings are associated with the elevation angle, θ_E, between the satellite and the ground station. Calculations of P_T are carried out for a range of elevation angles from 10° to 90°, while the altitude of the satellite, h_S, is maintained at 500 km. When the elevation angle, θ_E, is at 90°, it signifies that the satellite is directly overhead the ground station, resulting in a slant distance d_{GS} equal to $h_S - h_E$. The findings presented in Table

h_S (km)	d_{GS} (km)	L_{PG} (dB)	I_m (dB)	I_g (dB)	L_A (dB)	P_T (dBm)
100	152.4	-241.84	-0.15	-0.33	-0.48	-0.54
200	303.2	-247.81	-0.15	-0.33	-0.48	5.44
300	451.2	-251.27	-0.15	-0.33	-0.48	8.89
400	596.7	-253.69	-0.15	-0.33	-0.48	11.32
500	739.9	-255.56	-0.15	-0.33	-0.48	13.19
600	881.0	-257.08	-0.15	-0.33	-0.48	14.70
700	1020.1	-258.35	-0.15	-0.33	-0.48	15.98
800	1157.5	-259.45	-0.15	-0.33	-0.48	17.07
900	1293.2	-260.41	-0.15	-0.33	-0.48	18.04
1000	1427.4	-261.27	-0.15	-0.33	-0.48	18.90

Table 3: Slant distance vs. transmission power

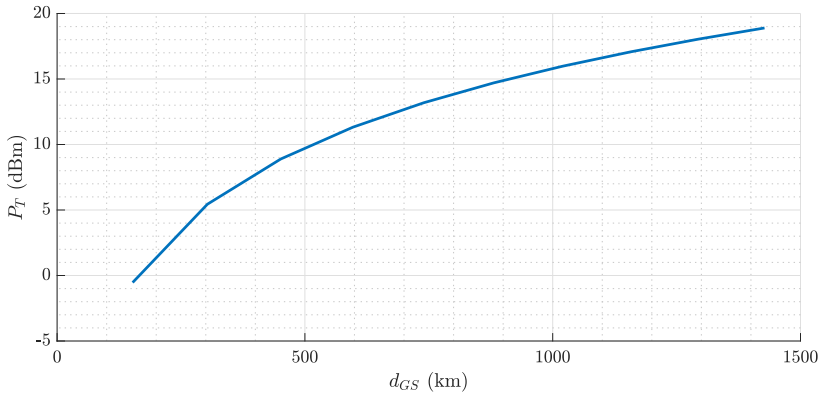

Figure 5: Slant distance vs. transmission power

4 and Figure 6 illustrate that P_T diminishes as θ_E increases.

θ_E (deg)	d_{GS} (km)	L_{PG} (dB)	I_m (dB)	I_g (dB)	L_A (dB)	P_T (dBm)
10	1692.7	-262.75	-0.57	-1.22	-1.79	21.68
20	1191.0	-259.70	-0.29	-0.62	-0.91	17.75
30	907.8	-257.34	-0.20	-0.42	-0.62	15.10
40	739.9	-255.56	-0.15	-0.33	-0.48	13.19
50	635.5	-254.24	-0.13	-0.28	-0.41	11.79
60	569.4	-253.29	-0.11	-0.24	-0.36	10.79
70	528.5	-252.64	-0.11	-0.22	-0.33	10.11
80	506.1	-252.26	-0.10	-0.21	-0.32	9.72
90	499	-252.14	-0.10	-0.21	-0.31	9.59

Table 4: Elevation angle vs. transmission power

3.4 Link Margin vs. Transmission Power

Table 5 presents the calculated values of P_T corresponding to various levels of LM and d_{SS}. For a specified d_{SS} within this table, an increase in LM leads to a higher P_T. The analysis also explores the requisite LM values corresponding to a given P_T across diverse

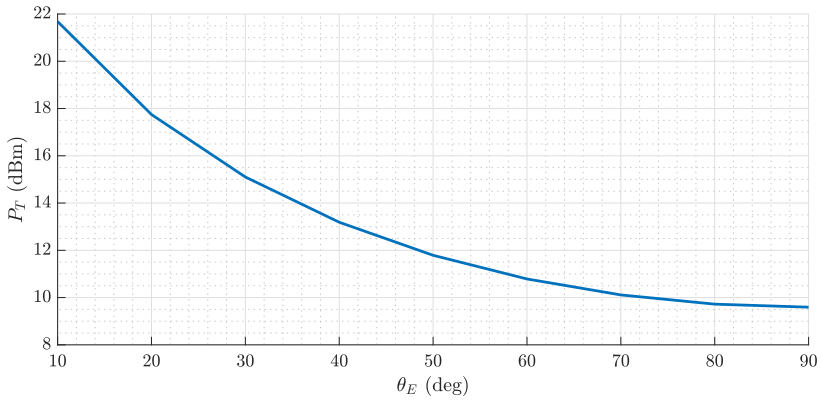

Figure 6: Elevation angle vs. transmission power

link distances. In the context of optical inter-satellite links, the study determines the feasible LM for establishing a connection between satellites when P_T is fixed at 1 W for different d_{SS} values. It is noted that the P_T for Mynaric's laser communication terminal does not exceed 1 W, as referenced in source [14].

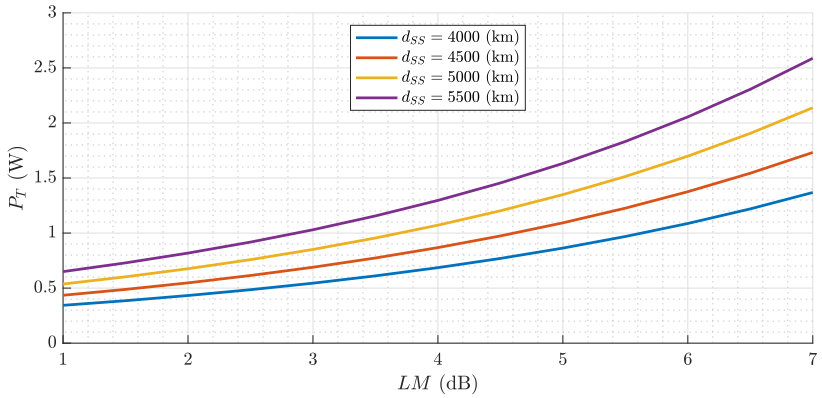

Figure 7: Link margin vs. transmission power

4 Discussion

For both optical inter-satellite links and optical uplinks/downlinks, the power transmission, P_T, exhibits an increase in conjunction with the growth of the slant distances, d_{GS}. This correlation highlights the strategic significance of satellite positioning to enhance operational longevity. It has been observed that the P_T requisite for optical uplinks/downlinks exceeds that of optical inter-satellite links for equivalent link distances. To illustrate, at a link distance of 1,000 km, the P_T for optical inter-satellite connectivity stands at 15.5 dBm, while optical uplinks/downlinks demand a P_T of 18.9 dBm.

Moreover, in the context of optical uplinks/downlinks, factors such as I_m and I_g, and subsequently L_A, are influenced by the elevation angle, θ_E. However, this influence is not uniform; L_A exhibits significant variations at smaller values of θ_E, with the rate of change diminishing markedly as θ_E increases. For instance, a notable alteration in L_A is observed

d_{SS} (km)	LM (dB)	P_R (dBm)	P_T (dBm)	P_T (W)
	4	-31.5	28.36	0.686
	4.5	-31.0	28.86	0.769
	5	-30.5	29.36	0.863
4000	5.5	-30.0	29.86	0.968
	6	-29.5	30.36	1.087
	6.5	-29.0	30.86	1.219
	7	-28.5	31.36	1.369
	4	-31.5	29.38	0.686
	4.5	-31.0	29.88	0.769
	5	-30.5	30.38	0.863
4500	5.5	-30.0	30.88	0.968
	6	-29.5	31.38	1.087
	6.5	-29.0	31.88	1.219
	7	-28.5	32.38	1.369
	2	-33.5	28.30	0.676
	2.5	-33.0	28.80	0.758
	3	-32.5	29.30	0.851
5000	3.5	-32.0	29.80	0.955
	4	-31.5	30.30	1.071
	4.5	-31.0	30.80	1.202
	5	-30.5	31.30	1.349
	1	-34.5	28.12	0.649
	1.5	-34.0	28.62	0.729
	2.0	-33.5	29.12	0.818
5500	2.5	-33.0	29.62	0.918
	3.0	-32.5	30.12	1.030
	3.5	-32.0	30.62	1.155
	4	-31.5	31.12	1.296

Table 5: Link margin vs. transmission power

when θ_E ascends from 10° to 20°, in contrast to the minimal shift from 70° to 80°.

As the slant distances, d_{GS}, extend at a constant power transmission, P_T, the link margin, LM, demonstrates a reciprocal trend, diminishing in response to the enlargement of d_{SS} and d_{GS}. This decrement in LM correlates with the amplification of L_{PS} and L_{PG}, which in turn diminishes the LM that can be sustained by a set P_T. Specifically for optical inter-satellite links, the available LM at a P_T of 1 W contracts as d_{SS} grows. Conversely, a greater LM is obtainable at lower satellite altitudes, h_S, hence a reduced d_{GS}, with a P_T of 1 W. However, this available LM tapers off as both h_S and d_{GS} increase for optical uplinks/downlinks.

5 Conclusion

This project explores the intricacies of optical inter-satellite links, focusing on essential aspects such as path loss, Doppler shift, atmospheric attenuation, and link margin. The mathematical models employed address the critical factors affecting satellite communication, including atmospheric conditions, satellite velocity, and elevation angles.

The analysis reveals a direct correlation between the increase in transmission power requirements and link distances, highlighting the importance of satellite positioning for communication efficiency. It also shows that optical uplinks/downlinks demand more transmission power than inter-satellite links for the same distances, pointing to the challenges in ground-to-satellite communications.

The examination of link margin versus transmission power uncovers an inverse relationship, underscoring the trade-offs between transmission power and link distance. This project illuminates the necessity of precise link budgeting to ensure reliable communication between satellites and between satellites and ground stations, emphasizing the balance needed for effective satellite communication systems.

References

[1] J. M. Gongora-Torres, C. Vargas-Rosales, A. Aragón-Zavala, and R. Villalpando-Hernandez, "Link budget analysis for LEO satellites based on the statistics of the elevation angle," *IEEE Access*, vol. 10, pp. 14518–14528, Jan 31 2022.

[2] I. Latachi, M. Karim, A. Hanafi, T. Rachidi, A. Khalayoun, N. Assem, S. Dahbi, and S. Zouggar, "Link budget analysis for a LEO cubesat communication subsystem," in *2017 International Conference on Advanced Technologies for Signal and Image Processing (ATSIP)*, pp. 1–6, May 22 2017.

[3] J. Liang, A. U. Chaudhry, E. Erdogan, and H. Yanikomeroglu, "Link budget analysis for free-space optical satellite networks," in *2022 IEEE 23rd International Symposium on a World of Wireless, Mobile and Multimedia Networks (WoWMoM)*, pp. 471–476, Jun 14 2022.

[4] A. Guidotti, A. Vanelli-Coralli, A. Mengali, and S. Cioni, "Non-terrestrial networks: Link budget analysis," in *ICC 2020 - 2020 IEEE International Conference on Communications (ICC)*, pp. 1–7, Jun 7 2020.

[5] U. J. Lewark, J. Antes, J. Walheim, J. Timmermann, T. Zwick, and I. Kallfass, "Link budget analysis for future e-band gigabit satellite communication links (71–76 and 81–84 ghz)," *CEAS Space Journal*, vol. 4, pp. 41–46, Jun 2013.

[6] S. Arnon, "Performance of a laser μsatellite network with an optical preamplifier," *JOSA A*, vol. 22, pp. 708–715, Apr 1 2005.

[7] R. W. Heath Jr and A. Lozano, *Foundations of MIMO communication*. Cambridge University Press, Dec 6 2018.

[8] H.-C. Lim, J. U. Park, M. Choi, C.-S. Choi, J.-D. Choi, J. Kim, *et al.*, "Performance analysis of dpsk optical communication for LEO-to-ground relay link via a geo satellite," *Journal of Astronomy and Space Sciences*, vol. 37, pp. 11–18, Jan 31 2020.

[9] S. Cakaj, B. Kamo, V. Koliçi, and O. Shurdi, "The range and horizon plane simulation for ground stations of low earth orbiting (LEO) satellites.," *Int. J. Commun. Netw. Syst. Sci.*, vol. 4, pp. 585–589, Sep 20 2011.

[10] I. Recommendation, "618-10 propagation data and prediction methods required for the design of earth-space telecommunication systems," *ITU-R Recommendations*, Jul 2003.

[11] M. S. Awan, E. Leitgeb, B. Hillbrand, F. Nadeem, M. Khan, *et al.*, "Cloud attenuations for free-space optical links," in *2009 International workshop on satellite and Space communications*, pp. 274–278, IEEE, Sep 9 2009.

[12] Z. Ghassemlooy, W. Popoola, and S. Rajbhandari, *Optical wireless communications: system and channel modelling with Matlab®*. CRC press, Apr 30 2019.

[13] E. Erdogan, I. Altunbas, G. K. Kurt, M. Bellemare, G. Lamontagne, and H. Yanikomeroglu, "Site diversity in downlink optical satellite networks through ground station selection," *IEEE Access*, vol. 9, pp. 31179–31190, Feb 16 2021.

[14] C. Carrizo, M. Knapek, J. Horwath, D. D. Gonzalez, and P. Cornwell, "Optical inter-satellite link terminals for next generation satellite constellations," in *Free-Space Laser Communications XXXII*, vol. 11272, pp. 8–18, SPIE, Mar 2 2020.

[15] B. Patnaik and P. K. Sahu, "Inter-satellite optical wireless communication system design and simulation," *IET Communications*, vol. 6, pp. 2561–2567, Nov 6 2012.

[16] A. Maho, M. Faugeron, A. Le Kernec, K. Elayoubi, and M. Sotom, "Assessment of the effective performance of dpsk vs. ook in satellite-based optical communications," in *International Conference on Space Optics—ICSO 2018*, vol. 11180, pp. 2101–2107, SPIE, Jul 12 2019.

[17] F. SpaceX, "update, nov. 2018,"spacex non-geostationary satellite system, attachment a, technical information to supplement schedule s,"," Nov 2018.

[18] H. Guo, B. Luo, Y. Ren, S. Zhao, and A. Dang, "Influence of beam wander on uplink of ground-to-satellite laser communication and optimization for transmitter beam radius," *Optics letters*, vol. 35, pp. 1977–1979, Jun 15 2010.

[19] Z. Xu, Y. Gao, G. Chen, R. Fernandez, V. Basavarajappa, and R. Tafazolli, "Enhancement of satellite-to-phone link budget: An approach using distributed beamforming," *IEEE Vehicular Technology Magazine*, vol. 18, pp. 85–93, Oct 16 2023.

[20] E. Kang, W. Shin, Y. Park, Y. B. Park, J. Kim, and H. Choo, "Link budget analysis of low earth orbit satellites considering antenna patterns and wave propagation in interference situations," in *2022 International Symposium on Antennas and Propagation (ISAP)*, pp. 511–512, Oct 31 2022.

MATLAB Code

```
clc; clear; close all;
set(groot,'defaultAxesTickLabelInterpreter','latex');
set(groot,'defaulttextinterpreter','latex');
set(groot,'defaultLegendInterpreter','latex');
set(groot,'defaultAxesFontSize',13);

%% FSPL Validation
D = 10e3:500e3; % distance in m
frequency = [145e6 435e6 1e9]; % frequency in Hz, e.g., 2.4 GHz for Wi-Fi
c = 3e8; % speed of light in vacuum in m/s
lambda = c ./ frequency; % calculate wavelength

FSPL_linear = FSPL(D, lambda);
FSPL_dB = linear2dB(FSPL_linear);

fig = figure;clf;
fig.Position = [50 50 700 300];
hold on;grid on;grid minor;
plot(D/(10^3), FSPL_dB(:,1), 'LineWidth', 2, 'DisplayName',...
'VHF');
plot(D/(10^3), FSPL_dB(:,2), 'LineWidth', 2, 'DisplayName',...
'UHF');
plot(D/(10^3), FSPL_dB(:,3), 'LineWidth', 2, 'DisplayName',...
'L-band');
xlabel('$d_{SS}$ (km)');
ylabel('Free Space Loss (dB)');
legend('show','Location','best');
set(gcf,'renderer','painters')
print(fig, 'FSPL_Val.eps', '-depsc2');

%% Doppler Validation
alpha = deg2rad(0:180);   % elevation angle
R = 6371000 + 500000; % Earth's radius plus the satellite's altitude m
Vc = 7500; % Velocity of the satellite in m/s
h = 500e3; % Altitude of the satellite above Earth's surface in meters

fdopp_VHF = DopplerShift(Vc, frequency(1), R, alpha, h, c);
fdopp_UHF = DopplerShift(Vc, frequency(2), R, alpha, h, c);
fdopp_Lband = DopplerShift(Vc, frequency(3), R, alpha, h, c);

fig = figure;clf;
fig.Position = [50 50 700 300];
hold on;grid on;grid minor;
plot(rad2deg(alpha), fdopp_VHF / 10^3, 'LineWidth', 2, 'DisplayName',...
```

```
'VHF');
plot(rad2deg(alpha), fdopp_UHF / 10^3, 'LineWidth', 2, 'DisplayName',...
'UHF');
plot(rad2deg(alpha), fdopp_Lband / 10^3, 'LineWidth', 2, 'DisplayName',...
'L-band');
xlabel('Elevation Angle (deg)');
ylabel('Doppler shift (kHz)');
legend('show','Location','best');
set(gcf,'renderer','painters')
print(fig, 'Doppler_Val.eps', '-depsc2');

%% Optical Inter-Satellite Link vs. Transmission Power
lambda = 1550;  % Laser wavelength nm
eta_T = 0.8;    % Transmitter optical efficiency
eta_R = 0.8;    % Receiver optical efficiency
R_data = 10;    % Data rate Gbps
D_R = 80;   % Receiver telescope diameter mm
theta_T = 1;    % Transmitter pointing error murad
theta_R = 1;    % Receiver pointing error murad
Theta_T = 15;   % Full transmitting divergence angle murad
P_req_linear = dBm2linear(-35.5);  % Receiver sensitivity w
bit_error_rate = 10^-12;
LM = dB2linear(3); % Link margin
P_R = LM * P_req_linear;

D = 1000:1000:10000;    % km
L_PS_linear = FSPL(D * 10^3, lambda * 10^-9);
L_PS_dB = linear2dB(L_PS_linear);
P_T_linear = optical_links(lambda, eta_T, eta_R, D_R,...
theta_T, theta_R, Theta_T, P_R,...
L_PS_linear);
P_T_dBm = linear2dBm(P_T_linear);

fig = figure;clf;
fig.Position = [50 50 700 300];
hold on;grid on;grid minor;
plot(D, P_T_dBm, 'LineWidth', 2);
xlabel('$d_{SS}$ (km)');
ylabel('$P_T$ (dBm)');
set(gcf,'renderer','painters')
print(fig, 'D_vs_P_T.eps', '-depsc2');

fig = figure;clf;
fig.Position = [50 50 700 300];
hold on;grid on;grid minor;
plot(D, L_PS_dB, 'LineWidth', 2);
```

```
xlabel('$d_{SS}$ (km)');
ylabel('$L_{PS}$ (dB)');
set(gcf,'renderer','painters')
print(fig, 'D_vs_L_PS.eps', '-depsc2');

%% Atmospheric Attenuation Parameters
h_E = 1;    % Ground station height km
L_W = 0.5;  % Thin cirrus cloud concentration cm^-3
N = 3.128 * 10^-4;  % Liquid water content g/m^-3
phi = 1.6;  % Partial size coefficient
theta_E = 40;   % Elevation angle deg
h_A = 20;   % Troposphere layer height km
R_E = 6378.1;   % radius of the Earth km
h_S = 100:100:1000; % altitude of the satellites km

d_GS = slant_distance(R_E, h_E, h_S, theta_E);  % Slant distance

L_PG_linear = FSPL(d_GS * 10^3, lambda * 10^-9);
L_PG_dB = linear2dB(L_PG_linear);

I_m_linear = mie_scattering(h_E, lambda * 10^-3, theta_E);
I_m_dB = linear2dB(I_m_linear);

I_g_linear = geo_scattering(L_W, N, phi, lambda, h_A, h_E, theta_E);
I_g_dB = linear2dB(I_g_linear);

L_A_dB = I_m_dB + I_g_dB;
L_A_linear = dB2linear(L_A_dB);

P_T_linear = optical_links_atm_atten(lambda, eta_T, eta_R, D_R,...
theta_T, theta_R, Theta_T, P_R,...
L_A_linear, L_PG_linear);
P_T_dBm = linear2dBm(P_T_linear);

fig = figure;clf;
fig.Position = [50 50 700 300];
hold on;grid on;grid minor;
plot(d_GS, P_T_dBm, 'LineWidth', 2);
xlabel('$d_{GS}$ (km)');
ylabel('$P_T$ (dBm)');
set(gcf,'renderer','painters')
print(fig, 'd_GSvs_P_T.eps', '-depsc2');

%% Elevation Angle vs. Transmission Power
theta_E = 10:10:90;
h_S = 500;
```

```
d_GS = slant_distance(R_E, h_E, h_S, theta_E);

L_PG_linear = FSPL(d_GS * 10^3, lambda * 10^-9);
L_PG_dB = linear2dB(L_PG_linear);

I_m_linear = mie_scattering(h_E, lambda * 10^-3, theta_E);
I_m_dB = linear2dB(I_m_linear);

I_g_linear = geo_scattering(L_W, N, phi, lambda, h_A, h_E, theta_E);
I_g_dB = linear2dB(I_g_linear);

L_A_dB = I_m_dB + I_g_dB;
L_A_linear = dB2linear(L_A_dB);

P_T_linear = optical_links_atm_atten(lambda, eta_T, eta_R, D_R,...
theta_T, theta_R, Theta_T, P_R,...
L_A_linear, L_PG_linear);
P_T_dBm = linear2dBm(P_T_linear);

fig = figure;clf;
fig.Position = [50 50 700 300];
hold on;grid on;grid minor;
plot(theta_E, P_T_dBm, 'LineWidth', 2);
xlabel('$\theta_E$ (deg)');
ylabel('$P_T$ (dBm)');
set(gcf,'renderer','painters')
print(fig, 'theta_Evs_P_T.eps', '-depsc2');

%% Link Margin vs. Transmission Power
LM_dB = 1:0.5:7;
LM_linear = dB2linear(LM_dB);
P_R_linear = received_power(LM_linear, P_req_linear);
P_R_dBm = linear2dBm(P_R_linear);

D = 4000:500:5500;    % km
P_T_dBm = zeros(length(LM_dB), length(D));

for i = 1:length(D)
L_PS_linear = FSPL(D(i) * 10^3, lambda * 10^-9);
L_PS_dB = linear2dB(L_PS_linear);
P_T_linear = optical_links(lambda, eta_T, eta_R, D_R,...
theta_T, theta_R, Theta_T, P_R_linear,...
L_PS_linear);
P_T_dBm(:,i) = linear2dBm(P_T_linear);
end
```

```
fig = figure;clf;
fig.Position = [50 50 700 300];
hold on;grid on;grid minor;
plot(LM_dB, dBm2linear(P_T_dBm(:,1)), 'LineWidth', 2, 'DisplayName',...
'$d_{SS} = 4000$ (km)');
plot(LM_dB, dBm2linear(P_T_dBm(:,2)), 'LineWidth', 2, 'DisplayName',...
'$d_{SS} = 4500$ (km)');
plot(LM_dB, dBm2linear(P_T_dBm(:,3)), 'LineWidth', 2, 'DisplayName',...
'$d_{SS} = 5000$ (km)');
plot(LM_dB, dBm2linear(P_T_dBm(:,4)), 'LineWidth', 2, 'DisplayName',...
'$d_{SS} = 5500$ (km)');
xlabel('$LM$ (dB)');
ylabel('$P_T$ (W)');
legend('show','Location','best');
set(gcf,'renderer','painters')
print(fig, 'LM_P_T.eps', '-depsc2');
%% Functions
function dB = linear2dB(linearValue)
% Check if the input is non-negative since power values can't be negative
if linearValue < 0
error('Input must be a non-negative value');
end

% Calculate the dB value from the linear scale input
dB = 10 * log10(linearValue);
end

function dBm = linear2dBm(linearPowerWatts)
% Ensure the power value is non-negative since power can't be negative
if linearPowerWatts < 0
error('Input power must be a non-negative value in Watts.');
end

% Convert the linear power in Watts to dBm
dBm = 10 * log10(linearPowerWatts) + 30;
end

function linearPowerWatts = dBm2linear(dBm)
% Convert the dBm value to linear power in Watts
linearPowerWatts = 10.^((dBm - 30) ./ 10);
end

function linear = dB2linear(dB)
% Convert the dB value to a linear scale
linear = 10.^(dB ./ 10);
```

```
end


function FSPL_linear = FSPL(D, lambda)

% calculateFSPL calculates the Free Space Path Loss (FSPL)
% D is the distance between the transmitter and receiver in meters
% lambda is the wavelength of the signal in meters

% Calculate FSPL in dB
for i = 1:length(lambda)
FSPL_linear(:,i) = (lambda(i) ./ (4 * pi * D)).^2;
end
end

function fdopp = DopplerShift(Vc, f, R, alpha, h, c)

% Calculate Doppler shift
for i = 1:length(alpha)
fdopp(i) = (Vc * f / c) * (R * cos(alpha(i))) / (R + h);
end
end

function P_R = received_power(LM, P_req)

P_R = LM * P_req;
end

function P_T = optical_links(lambda, eta_T, eta_R, D_R,...
theta_T, theta_R, Theta_T, P_R,...
L_PS)

% lambda = Laser wavelength mm
% eta_T = Transmitter optical efficiency
% eta_R = Receiver optical efficiency
% R_data = Data rate Gbps
% D_R = 80 Receiver telescope diameter mm
% theta_T = 1 Transmitter pointing error murad
% theta_R = 1 Receiver pointing error murad
% Theta_R = 15 Full transmitting divergence angle murad
% P_req = -35.5 Receiver sensitivity dBm

% The transmitter gain
G_T = 16 / (Theta_T)^2;

% The receiver gain
```

```
G_R = (D_R * pi / lambda)^2;

% The transmitter pointing loss
L_T = exp(-G_T * (theta_T)^2);

% The receiver pointing loss
L_R = exp(-G_R * (theta_R)^2);


den = eta_T * eta_R * G_T * G_R * L_T * L_R .* L_PS;
P_T = P_R ./ den;
P_T = P_T * 10^-24;  % watts
end

function d_GS = slant_distance(R_E, h_E, h_S, theta_E)
% R_E = radius of earth km
% h_E = height of ground station km
% h_S = altitude of the satellites km
% theta_E = elevation angle deg

theta_E = deg2rad(theta_E);
R = R_E + h_E;
H = h_S - h_E;
A = ((R + H) ./ R).^2;
B = (cos(theta_E)).^2;
C = sin(theta_E);

d_GS = R .* (sqrt(A - B) - C);

end

function I_m = mie_scattering(h_E, lambda, theta_E)

% lambda = micrometers

theta_E = deg2rad(theta_E);
a = -0.000545 * lambda^2 + 0.002 * lambda - 0.0038;
b = 0.00628 * lambda^2 - 0.0232 * lambda + 0.00439;
c = -0.028 * lambda^2 + 0.101 * lambda - 0.18;
d = -0.228 * lambda^3 + 0.922 * lambda^2 - 1.26 * lambda + 0.719;

rho = a * (h_E)^3 + b * (h_E)^2 + c * (h_E) + d;
I_m = exp(-rho ./ sin(theta_E));

end
```

```
function I_g = geo_scattering(L_W, N, phi, lambda, h_A, h_E, theta_E)

% lambda = nm
% L_W = liquid water content g/m^-3
% N = cloud number concentration cm^-3

% visibility in km
V = 1.002 / (L_W * N)^0.6473;

% attenuation coefficient
theta_A = (3.91 / V) * (lambda / 550)^(-phi);

% distance of the optical beam through the...
% troposphere layer of the atmosphere
d_A = (h_A - h_E) .* csc(deg2rad(theta_E));

I_g = exp(-theta_A .* d_A);

end

function P_T = optical_links_atm_atten(lambda, eta_T, eta_R, D_R,...
theta_T, theta_R, Theta_T, P_R,...
L_A, L_PG)

% lambda = Laser wavelength mm
% eta_T = Transmitter optical efficiency
% eta_R = Receiver optical efficiency
% R_data = Data rate Gbps
% D_R = 80 Receiver telescope diameter mm
% theta_T = 1 Transmitter pointing error murad
% theta_R = 1 Receiver pointing error murad
% Theta_R = 15 Full transmitting divergence angle murad
% P_req = -35.5 Receiver sensitivity dBm

% The transmitter gain
G_T = 16 / (Theta_T)^2;

% The receiver gain
G_R = (D_R * pi / lambda)^2;

% The transmitter pointing loss
L_T = exp(-G_T * (theta_T)^2);

% The receiver pointing loss
L_R = exp(-G_R * (theta_R)^2);
```

```
den = eta_T * eta_R * G_T * G_R * L_T * L_R .* L_A .* L_PG';
P_T = P_R ./ den;
P_T = P_T * 10^-24;  % watts

end
```